An Investigation of Numerical Grid Effects in Parameter Estimation

by George A. Zyvoloski[1] and Velimir V. Vesselinov[2]

Abstract

Modern ground water characterization and remediation projects routinely require calibration and inverse analysis of large three-dimensional numerical models of complex hydrogeological systems. Hydrogeologic complexity can be prompted by various aquifer characteristics including complicated spatial hydrostratigraphy and aquifer recharge from infiltration through an unsaturated zone. To keep the numerical models computationally efficient, compromises are frequently made in the model development, particularly, about resolution of the computational grid and numerical representation of the governing flow equation. The compromise is required so that the model can be used in calibration, parameter estimation, performance assessment, and analysis of sensitivity and uncertainty in model predictions. However, grid properties and resolution as well as applied computational schemes can have large effects on forward-model predictions and on inverse parameter estimates. We investigate these effects for a series of one- and two-dimensional synthetic cases representing saturated and variably saturated flow problems. We show that "conformable" grids, despite neglecting terms in the numerical formulation, can lead to accurate solutions of problems with complex hydrostratigraphy. Our analysis also demonstrates that, despite slower computer run times and higher memory requirements for a given problem size, the control volume finite-element method showed an advantage over finite-difference techniques in accuracy of parameter estimation for a given grid resolution for most of the test problems.

Introduction

The motivation for this work is from the authors' experience in the Yucca Mountain (Nevada) and Espanola Basin (New Mexico) projects. Large three-dimensional numerical models exist for ground water flow in both the unsaturated and saturated zone at the Yucca Mountain potential repository area (Zyvoloski et al. 2003; Liu et al. 2003). A large basin-scale numerical model also exists for the Espanola Basin (Keating et al. 2003). These models are used to provide quantitative estimates of water flow and potential contaminant transport in the subsurface. Computer models of similar complexity exist for the large

remediation efforts at the Savannah River (Flach et al. 1996), Hanford (Cole et al. 1997), Cape Cod (e.g., Barlow 1994), and the MADE site (e.g., Rehfeldt et al. 1992), to name just a few. Though these sites may occur in different hydrogeologic settings, the settings themselves are complicated and may include many different hydrogeologic units through which fluids and contaminates can flow, and also the possibility of flow and transport through different portions of the medium (double porosity/double permeability) at different spatial and temporal scales. The purpose of these models is to predict an unknown state of the system in the past or the future, e.g., time at which a contaminant will reach a compliance boundary or contaminant concentrations will exceed the EPA standard at some observation well. The quantitative nature of this analysis requires the evaluation of errors and uncertainties associated with the models.

There are various types of uncertainty associated with the model predictions. The uncertainties can be categorized into three groups related to three different aspects (steps) of model development: conceptual model,

[1]Corresponding author: Earth and Environmental Sciences Division, Los Alamos National Laboratory, Los Alamos, NM 87545; gaz@lanl.gov

[2]Earth and Environmental Sciences Division, Los Alamos National Laboratory, Los Alamos, NM 87545; vvv@lanl.gov

representation of the conceptual model in the numerical model, and model parameters. There is a long list of publications related to the uncertainties associated with model parameters (cf. McLaughlin and Townley 1996; de Marsily et al. 2000; and references therein). Recently, there have also been attempts to address the conceptual model component in the uncertainty of model predictions (e.g., Gaganis and Smith 2001; Neuman 2003). In this study, we investigate the impact of numerical representation of the conceptual model, particularly the impact of the grid properties and resolution. In advective-dispersive transport simulations, numerical dispersion is proportional, in simple upwinding schemes, to the size of grid cells. Less intuitive are errors associated with the flow solution and representation of permeability or topographic structure. Sinton (1998), for example, found considerable differences in the numerical flow solutions when a problem with dipping hydrostratigraphy is solved using computational grids of different resolution. In contrast to the other sources of uncertainty, the model uncertainty associated with numerical grid errors can often be dealt with a priori.

The computational grid errors are associated with numerical grid resolution, the representation of permeability structure on a numerical grid, and differencing method used. These errors can be interrelated. For example, in an effort to represent a spatially varying permeability structure on a relatively coarse grid (CG), conformable (also called "deformable") layers can be used (McDonald and Harbaugh 1988; Kautsky et al. 2001; Lemon and Jones 2001). This technique compromises the accuracy and convergence properties of the applied numerical difference scheme because it employs finite-difference (FD) cells with variable vertical thickness to approximate the variable thickness of hydrostratigraphic units with structured grids (structured grids use a constant number of cells in all the Cartesian coordinates). The scheme assumes that the computational grid is orthogonal and therefore it does not account for the additional terms associated with nonorthogonal grids. Although the conforming FD scheme allows for a better representation of the model domain and properties, it introduces numerical errors associated with the missing (nonorthogonal) parts of the differencing scheme when used with an FD code like MODFLOW (McDonald and Harbaugh 1988). This limitation in MODFLOW is explicitly mentioned in the manual (McDonald and Harbaugh

1988, 2–31) but rarely taken into account. Thus, these conformable schemes seem to improve the representational error associated with the permeability structure while introducing a numerical differencing error. This is different from the truncation error associated with grid size and contains a component proportional to the deviation of the grid from being orthogonal. The errors induced by conforming grids were previously studied by Weiss (1985), Harte (1994), Hoagland and Pollard (2003), and Bower et al. (2004). They concluded that the appropriate grid size could be determined a priori for a given problem. To evaluate the usefulness of "conformable layers," it is important to understand the errors associated with this emerging technology and how the grid angle affects the results.

Examples of structured grids are presented in Figure 1. Figure 1a shows an orthogonal computational grid applied to represent flow to a well through a layered domain. Figure 1b shows a nonorthogonal grid representation applied to represent complex geometry of various hydrostratigraphic units. Here, the grid cells lack the orthogonality to support the standard 5-point FD stencil. Note the steep slopes of the boundaries separating different hydrostratigraphic units.

There are various techniques and software packages for mapping the geological models on the computation grids as done in Figure 1. For MODFLOW, popular packages are T-PROGS, HUF, GMS, and VisualMODFLOW. Another approach is to use the code LaGriT (George et al. 1999), which uses various techniques to map the geologic model on the computational grid. The geologic model is constructed using StrataModel, EarthVision or other similar programs. The latter approach is commonly used in numerical models based on finite-element heat and mass (FEHM).

It is important to note that even though sometimes ignored in regional ground water modeling studies, unsaturated flow and transport can be important to saturated flow and transport. Ground water recharge and contaminant flowpaths are frequently associated with flow and transport through an unsaturated zone. The errors discussed previously are important in large-scale problems in the saturated zone largely because of the complexity, on a basin scale, of the permeability. These errors may be even more important in near–ground surface applications where the topographic, unsaturated flow and phreatic aquifer effects can lead to unreasonable compromises being made in grid generation and numerical methods.
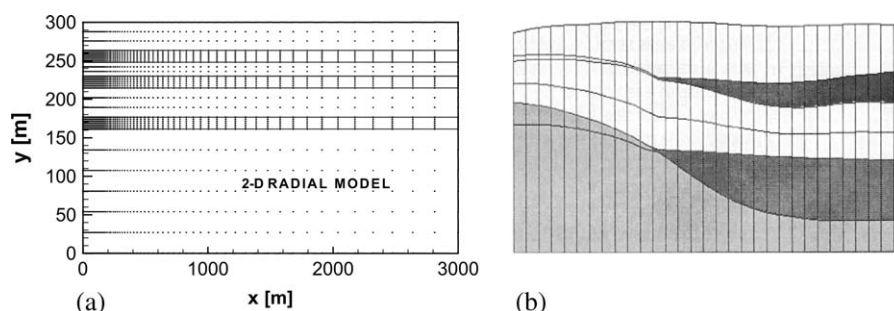

(a)   (b)

Figure 1. Examples of grids where resolution and discretization method are important: (a) radial flow to a well, (b) conforming grid blocks (Lemon and Jones 2001).

That is why in this study we also investigate the impact of the computational grid on flow and transport through variably saturated media as well. The analysis is performed using two-phase flow simulations, but a similar impact can be expected if the simulations were performed for the saturated flow only but taking into account the water table movement (as it can be performed in codes such as FREESURF [Neuman and Witherspoon 1970; Neuman 1976] and MODFLOW [using the wetting/drying package]).

In this study, we demonstrate the impact of grid properties and resolution on the inverse estimates of model parameters and the respective model predictions. We do this for a series of one- and two-dimensional synthetic cases. We make conclusions about the grids that should be preferred in the model development. We also rank the errors associated with numerical grid resolution and differencing method based on their impact on the inverse estimates. The proposed methodology can be used to test the impact of grid resolution on the inverse model parameter estimates before the model is calibrated to the real data.

To address the impact of grid effects on the model results, it is also possible to analyze only what is the impact of the differences in the grid resolution on the forward-model solutions. However, in practice, it is much more important to analyze how the errors associated with the grid effects impact the respective inverse estimates.

Methodology

To investigate the grid effect, we perform a series of inverse analyses (parameter estimation) estimating model parameters. Different inverse analyses use different grid resolution and computational schemes. We evaluate the impact of grid effects by comparing estimated model parameters and the "true" parameter values. The calibration targets for the inverse analyses are obtained using the true parameter values in numerical models with very fine grids (VFGs). We also compare respective forward-model predictions based on the different calibrated models. We analyze one- and two-dimensional problems for fully saturated and variably saturated (saturated/unsaturated) flow. The computer codes used in the study are the control volume FEHM transfer code (Zyvoloski et al. 1997)

and the automated parameter estimation code PEST (Doherty 2000). The code FEHM uses finite-volume and finite-element computational techniques with general unstructured grids. The finite-volume capability allows the code to be used to solve FD and conforming finite-difference (CFD) grids as well. In these cases, the major difference between MODFLOW and FEHM is that FEHM does not account for the structured nature of the grid and solves the problem as if the grid is unstructured. This increases the computational time and memory requirements when compared to MODFLOW.

The computational (differencing) schemes analyzed in our study are presented in Figure 2. The standard FD method is shown in a context of sloping hydrostratigraphic units (Figure 2a). Also shown is an example for application of the conforming CFD formulation to represent the sloping layer (Figures 2b). Even though the method allows for tracking on complex spatial hydrostratigraphy (as also shown in Figure 1b), it is mathematically inaccurate. It introduces a systematic error proportional to the grid angle, and this error persists regardless of the grid resolution. CFD formulations are available in many FD ground water flow computer codes, including MODFLOW. The control volume finite-element (CVFE) method for a sloping layer is shown in Figure 2c. This method can accurately represent complex stratigraphy and is mathematically convergent and does not introduce systematic errors due to missing connections (Forsyth 1989). The drawback for the CVFE method is that it contains more connections, ~50% more for the examples given here, and thus uses more computer memory and time to complete the simulations. For unsaturated zone simulations, the nonlinearities of the relative permeability require a positive connection term for numerical stability of the upwinding scheme. In a vertical plane with a slanted grid following a sloping geologic contact, the easiest way to ensure positive connection terms is to use the CFD stencil and thus simply ignore any additional terms that would arise from the nonorthogonal nature of the grid. The numerical truncation error in this approach is proportional to the grid angle and would appear to be small only for gently sloping units. The CVFE scheme adds the necessary connections while ensuring positive connection terms assuming certain grid constraints are met.
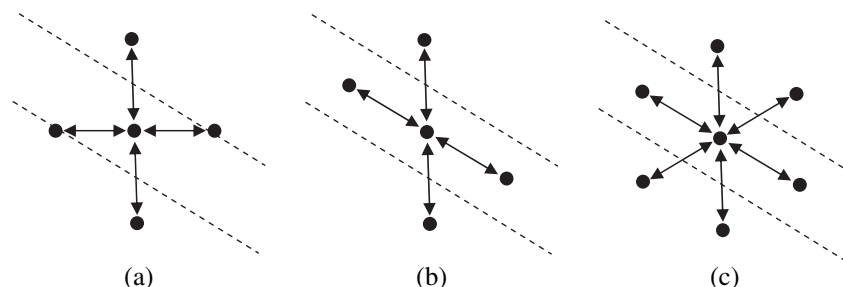

Figure 2. Difference stencils used for representation of layered hydrostratigraphy: (a) FD, (b) CFD in case of sloping layers, and (c) CVFE.

The discrete equations that describe the material balance equations are the same for FD, CVFE, and CFD formulations (shown here for water):

$$V_i \frac{\left[(\rho\phi)^{n+1} - (\rho\phi)^n\right]}{\Delta t} = \sum_{\text{neighbor cells}} \left(\frac{k\rho}{\mu}\right)_{ij} \left(\frac{A_{ij}}{\Delta d_{ij}}\right) \left[(P_j - P_i) - (\rho g)_{ij}(z_j - z_i)\right] \tag{1}$$

Where V is the control volume, A is the facet area, d is the internodal distance, and z is the elevation. The symbols i and j refer to the grid block and neighbor nodes, respectively. Additionally, g is the acceleration due to gravity, ρ is density, ϕ is porosity, P is pressure, μ is viscosity, Δt is the time step size, and n refers to the time step level. Source or sink terms and boundary conditions will modify the previous equation.

Forsyth (1989) compares the FD and CVFE equations formulation. Each method requires a control volume with consistent and positive areas. For FD methods, control volumes are orthogonal rectangles or hexahedrals; all interface areas are well defined. The CVFE method, besides the FD control volumes, allows for triangular, tetrahedral, parallelogram, and nonorthogonal hexahedral control volumes. These control volumes have rules (e.g., the Voronoi or Delauney conditions) governing the facet angles in order to produce positive area coefficients. In particular, Young (1999) showed that a relationship exists between grid size in the coordinate directions and the grid slope to maintain positive face areas for corner terms. Rozon (1989) showed that the CVFE method produced the standard FD difference equations when applied to orthogonal grids. The corner terms in the analysis given by Young (1999) are missing in the CFD formulation. The size of these terms and indeed their sign is a function of grid angle. We note here that the traditional Finite Element scheme, with nodal connection terms computed from interpolation functions, have no inherent control on the sign of the connection terms. We note also that the flux continuous FD formulation of Lee et al. (1999) will automatically produce the additional connections for nonorthogonal dipping grids. The method, however, is not easily implemented in standard FD computer codes.

Test Models, Results, and Dicussion

One–Dimensional Saturated Radial Flow

To investigate the grid resolution effects, we analyze well test data using an inverse flow model. The numerical flow domain represents one-dimensional radial flow in the vicinity of an injection well. The model parameters are given in Table 1. The aquifer is confined with unknown permeability. The specific storage is assumed to be known. The transient changes in the hydraulic pressures are recorded at the injection well. The transient calibration targets are computed assuming permeability equal to 10^{-12} m^2, specific storage equivalent to water compressibility

Table 1 **Input Parameters for Radial Flow Problem**	
Problem size in X direction (radial geometry)	1000 m
Injection rate	2.2222×10^{-3} kg/s/m
Simulation time	1.0 d
Temperature	20°C
Initial pressure	1.0 MPa
Porosity	0.2
Specific storage	5.7×10^{-6} m^{-1}
Permeability (estimated)	1.0×10^{-12} m^{-2}
Grid resolution	Variable

(5.7×10^{-6} m^{-1}), and using a numerical model with a very fine one-dimensional radial grid. Eleven synthetic observation data points are generated representing transient pressures at radial position 0.05 m and times equal to 0.01, 0.02, 0.03, 0.05, 0.1, 0.2, 0.3, 0.4, 0.6, 0.8, and 1 d. Since we have used VFG, we do not expect to introduce numerical errors in the calibration targets. This numerical solution is within 1% of the equivalent Theis solution. The maximum drawdown at the well is 0.01 m; the imposed gradients are very small.

To examine the effect of grid resolution on permeability estimates, eight one-dimensional grids are studied. For all the grids the first grid block where the producing well is located equals 0.0005 m. The number of grid blocks range from 35 to 10,000 in the radial direction (Table 1). Four of the grids are geometrically spaced from 0.005 m spacing to large spacing and four are kept at constant spacing (except for the first grid block as explained previously). While it may seem obvious to use geometrical spacing for better accuracy in this example, the analysis here helps in the understanding of transient analysis and calibration in the context of a large model where it is difficult to use geometrical grid spacing near wells. In these cases, uniform grid spacing is commonly employed near the wells.

The results are presented in Table 2. All the inverse solutions produce good matches between observed and simulated transient pressures; the sum of squared residuals (SSR) for each of the calibrations is less than 10^{-4} m^2 (Table 2), i.e., smaller than the discrepancy between numerical and analytic solutions. The differences between the inverse estimates of permeability show the importance of grid resolution. If well-designed, geometrically spaced grids were used, the exact true permeability (10^{-12} m^2) could be reproduced within a few percent even on a fairly CG (cases 1 to 4 in Table 2). However, the evenly spaced grids produce estimates far lower than the "true" permeability (cases 5 through 8 in Table 2). It is important to note that in these cases, the estimation uncertainty reported by the parameter estimation code theoretically cannot account for the estimation error associated with the grid resolution. Even for the poorest estimate (case 5 in Table 2), the parameter estimation code is calculating low estimation errors for the parameters; the 95% confidence intervals on the estimate

Table 2
Permeability Estimates and Grid Characteristics for Radial Flow Problem

Case	Number of Nodes	Type of Node Distribution	Horizontal Length of Largest Grid Block (m)	Estimated Permeability ± 95% Confidence Intervals (m²)	SSR (m²)
1	35	Geometric	333	$0.965 \times 10^{-12} \pm 3.1 \times 10^{-16}$	4.3×10^{-6}
2	129	Geometric	91	$1.001 \times 10^{-12} \pm 8.8 \times 10^{-17}$	1.2×10^{-6}
3	439	Geometric	24	$1.000 \times 10^{-12} \pm 1.4 \times 10^{-17}$	1.8×10^{-7}
4	997	Geometric	10	$1.000 \times 10^{-12} \pm 1.3 \times 10^{-20}$	1.3×10^{-12}
5	100	Even	10.0	$0.261 \times 10^{-12} \pm 2.1 \times 10^{-14}$	9.5×10^{-4}
6	500	Even	2.0	$0.397 \times 10^{-12} \pm 1.5 \times 10^{-14}$	4.9×10^{-4}
7	1000	Even	1.0	$0.454 \times 10^{-12} \pm 1.4 \times 10^{-14}$	3.8×10^{-4}
8	10000	Even	0.1	$0.706 \times 10^{-12} \pm 6.9 \times 10^{-14}$	1.3×10^{-4}

are within only 5% of the estimated parameter value (Table 2). As it was suggested in the literature (e.g., Carrera 1984), a special care should be warranted when 95% confidence intervals are used to represent uncertainty in the model parameters. Commonly, the 95% confidence intervals reported by the parameter estimation code reflect only a particular source of uncertainty (in this case the measurement errors in the calibration targets and the quality of the obtained inverse matches). However, there are other sources of uncertainty not reflected in the analysis, and that is why often inverse results imply greater certainty than is warranted.

Two–Dimensional Saturated Flow in Layered Medium

Parameters for the layered problem are presented in Table 3. Figure 3 represents the flow domain, boundary conditions, spatial extent of the zones associated with different permeabilities, and location of the calibration targets. The sloping of the layers is approximately 5° (note the difference between horizontal and vertical scales in Figure 3). There is a steady-state, fully saturated (confined) flow from left to right through the model domain. There are 14 calibration targets representing the steady-state hydraulic pressure distributed through the domain. The calibration targets are computed numerically using

a VFG resolution (12.5- by 10-m grid size) and standard FD formulation. The problem is designed such that all the tested grids have nodes in close vicinity to the calibration target locations. Of note is the fact that there are two zones of relatively high permeability (zone 3 and zone 5) and two of relatively low permeability (zones 2 and 4); zone 1 is a no-flow domain represented as a low-permeability zone in the FD case. Permeabilities of zones 2, 3, and 4 are assumed to be unknown and estimated in the inverse process. Permeabilities of zones 1 and 5 are assumed to be known. The boundary conditions for this model consist of a distributed flux on the left side and a constant head on the right side. They are shown in Figure 3. The alternating high and low permeability of this model represents an idealization of a heterogeneous permeability field that exists in many regional scale flow systems.

Figure 4a shows a coarse orthogonal FD mesh with the hydrogeologic zones shown in Figure 3 mapped to the mesh. The grid depicted in Figure 4b represents the respective CFD formulation. This type of grid is used

Table 3
Parameters for Two-Dimensional Problem of Saturated Flow Through a Layered Medium

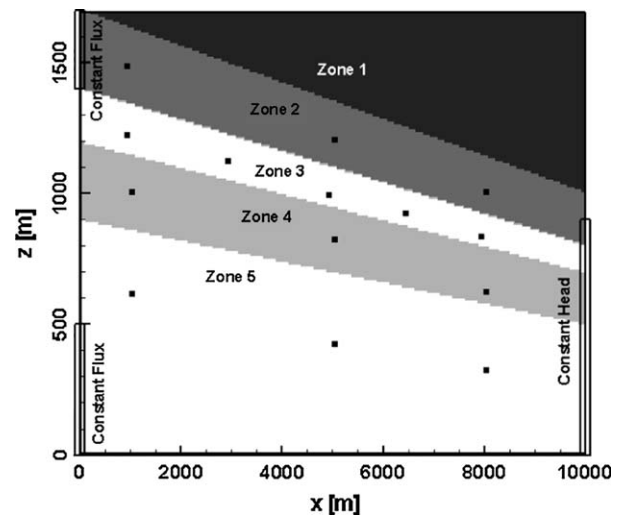|	
Problem size (m)	X direction 10,000
	Z direction 1700
Specified fluxes (inflow) (kg/s)	0.1 (inflow 1)
	0.2 (inflow 2)
Outflow head condition (m)	700
Permeabilities (m²)	1.0×10^{-14} (zone 2)
Very fine scale values	1.0×10^{-11} (zone 3)
	1.0×10^{-14} (zone 4)
Fixed permeabilities (m²)	1.0×10^{-18} (zone 1)
	5.0×10^{-13} (zone 5)
Grid resolution (m)	X direction 12.5
(very fine scale)	Z direction 10.0

Figure 3. Computational domain for two-dimensional saturated flow through layered medium. The small black squares show the location of calibration targets. Note the difference between horizontal and vertical scales; the vertical axis is exaggerated by a factor of ~5.
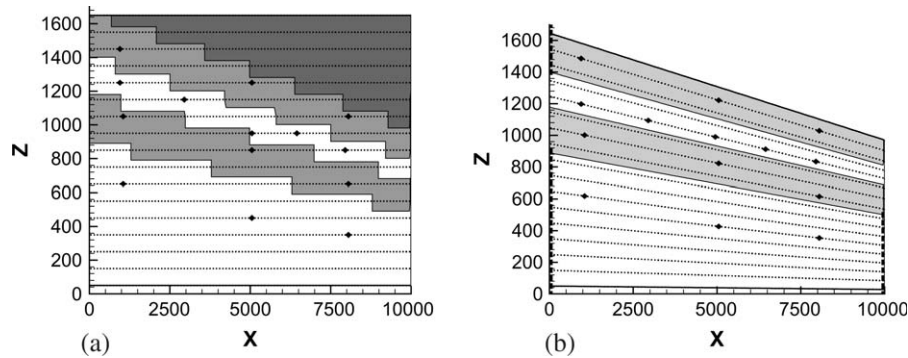
Figure 4. Grid representation for VCG case of the layered problem for (a) the FD and (b) CFD and CVFE formulations. Note the difference between horizontal and vertical scales; the vertical axis is exaggerated by a factor of ~5.

with codes allowing for variable vertical cell thickness, variable cell elevation, and nonorthogonal grid cells (e.g., MODFLOW). Even considering the exaggerated vertical scale, it is easy to see the motivation for using the CFD method. Figure 4b also represents the CVFE method. The grid cell spacing is very close to that shown for the CFD grid; small differences (not shown in Figure 4b) exist along the domain boundaries only where additional grid cell rows/columns are required so that the spacing of the CVFE and CFD grids can match accurately. Defining low permeability in zone 1 or inactivating grid blocks is required in the FD case to represent the no-flow domain. Zone 1 is not explicitly required or represented in the CFD and CVFE formulations where the bottom of zone 1 is defined as a no-flow boundary (Figure 4b).

The inverse results obtained using different grid resolutions and differencing techniques are given in Table 4 including the objective function (sum-squared of the residuals) estimates. Also given are the number of grid blocks and grid-block sizes. Based on resolution, the applied grids are divided into four groups: VFG (used to compute calibration targets), fine grid (FG), CG and very coarse grid (VCG). Grid convergence study assured that the solution changed with less than 1% when the grid resolution was changed by a factor of two. Therefore, we do not expect to introduce numerical errors in the calibration targets. The table presents the inverse permeability estimates for zones 2, 3, and 4. A comparison of the inverse

estimates shows that all the test cases (using different grid resolutions and differencing techniques) accurately identified the lower permeability at zones 2 and 4 and higher permeability at zone 3. Further, all the methods did relatively well in estimating the true permeability of zones 3 and 4, regardless of grid resolution. However, for the coarser grid (CG and VCG) cases, the FD method performs very poorly in estimation of the true permeability of zone 2. In these cases, the flow area of zone 2 and zone 3 is not resolved accurately by the computational grid, and as a result, the flow within zone 2 is substantially affected by the model's inability to flow in the high-permeability zone 3. To compensate for this effect, the estimated permeabilities are 20 to 80 times higher than the "truth" in zone 2 in order to match the calibration targets. These causes the high residual for one of the targets, located at $(x, z) = (1000\ m, 1000\ m)$ in Figure 3. This target accounts for 50% to 80% of the objective function in these two calibrations (Table 4). For reasons discussed previously, we believe the true high head at this observation point could not be achieved because of the diversion of fluid in zone 2.

It is important to note that for this problem, the accuracy of the inverse solution depends on the accurate representation of the geometry of hydrostratigraphic units rather than on the accurate mathematical formulation of the differencing scheme. This is a result of moderate sloping of the "conformable" layers, which is only 5%. The steeper is the slope, the higher are the errors.

Table 4
Permeability Estimates Obtained Using Different Grid Resolution and Differencing Techniques For a Two-Dimensional Saturated Flow Through a Layered Medium

Case	Grid	Method	Number of Grid Blocks	(DX, DZ) (m)	k (zone 2) (m²)	k (zone 3) (m²)	k (zone 4) (m²)	SSR (m²)
1	VFG	FD	136,000	(12.5, 10)	1.0×10^{-14} (truth)	1.0×10^{-11} (truth)	1.0×10^{-14} (truth)	N/A
2	FG	FD	27,200	(25, 25)	1.1×10^{-14}	1.0×10^{-11}	0.99×10^{-14}	2.42
3	CG	FD	1700	(100, 100)	$20. \times 10^{-14}$	1.0×10^{-11}	0.97×10^{-14}	126.3
4	CG	CFD	1700	(100, 100)	1.2×10^{-14}	0.98×10^{-11}	1.0×10^{-14}	0.193
5	CG	CVFE	1938	(100, 100)	1.2×10^{-14}	0.96×10^{-11}	0.96×10^{-14}	3.61
6	VCG	FD	850	(200, 100)	$84. \times 10^{-14}$	0.92×10^{-11}	0.95×10^{-14}	193.9
7	VCG	CFD	850	(200, 100)	1.8×10^{-14}	0.97×10^{-11}	0.95×10^{-14}	4.45
8	VCG	CVFE	988	(200, 100)	1.6×10^{-14}	1.0×10^{-11}	0.92×10^{-14}	7.92

Inaccurate estimation of permeability of the confining units will produce inaccuracy in posterior predictions of the contaminant transport through the confining layers to the highly permeable layers.

Two-Dimensional Saturated/Unsaturated Flow in Layered Medium

Parameters for the layered problem are presented in Table 5. Figure 5 shows the flow domain, boundary conditions, spatial extent of the zones associated with different permeabilities, and location of the calibration targets. As in the saturated zone section, the slope of the layers is about 5°. The flow is assumed to be at steady state. The steady-state calibration targets for hydraulic pressures are computed numerically using FG resolution (25-m horizontal spacing and 25-m vertical spacing) and standard FD formulation. The calibration set includes 16 pressures and 13 saturations (total number of targets is 29). The location and type of calibration targets are shown in Figure 5. The problem is designed in a way that all the tested grids have nodes associated with the locations of calibration targets. There are two zones of relatively high permeability (zone 1 and zone 3) and one of relatively low permeability (zone 2) separating the high-permeable zones. The permeabilities of all three zones are assumed unknown. The boundary conditions consist of fluid fluxes at the left side boundary in the upper (inflow 1) and lower (inflow 2) high-permeability zones and a seepage face condition on the right side boundary. This simplified model replicates regional flow in a deep aquifer, overlain with a confining layer with recharge from a local perched zone. If a contaminant source also exists in the perched zone, it is imperative to estimate all of the permeabilities accurately.

The inverse results obtained using different grid resolutions and differencing techniques are given in Table 6. Also given are the number of grid blocks and grid-block sizes. Based on resolution, the applied grids are divided
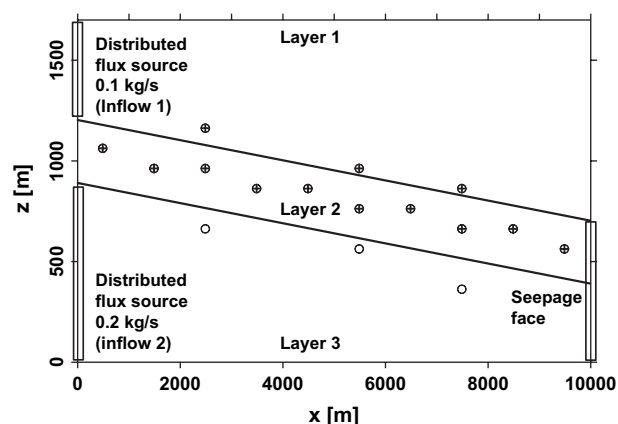

Figure 5. Computational domain for two-dimensional variably saturated flow through layered medium. Boundaries of the layers are shown with thick lines. The locations of pressure and saturation calibration targets are shown with open circles and crosses, respectively. Note the difference between horizontal and vertical scales; the vertical axis is exaggerated by a factor of ~5.

into three groups: VFG, FG, and CG. The calibration targets are estimates using the VFG FD solution. Different inverse solutions produce close matches of calibration targets; the objective function estimates (the SSR) are also listed in Table 6. The table presents the inverse permeability estimates for zones 1, 2, and 3. Figure 6 shows the distributions of water saturation (gray scale) and hydraulic pressure (MPa, lines) within the model domain for the calibrated solutions. The true ground water flow system is defined by the VFG FD solution (Figure 6a). Grid convergence study assured that the solution changed with less than 5% when the grid resolution was changed by a factor of 2. Therefore, we do not expect to introduce numerical errors in the calibration targets. The simulated water tables are defined by the 1-MPa contour line of hydraulic pressure. Note that a capillary fringe zone is simulated above the water table. In the right end of the model, the capillary fringe zone becomes perched zone (a shallow saturated zone separated by the deep saturated zone by unsaturated zone). Note that the model setup allows for ground water perching within zone 2. This is controlled by the property contrasts between zone 1 and zone 2 and between zone 2 and zone 3.

Table 6 demonstrates that for the same grid resolution (cases 3 to 5), we obtain different estimates using different differencing techniques. This is especially true for zone 1. Its permeability is overestimated by about 1 order of magnitude the FD method to allow for the unsaturated flow in this zone. The CFD method underestimates (~50%) the permeability of zone 1 to decrease the perched flow, which is otherwise systematically overestimated due to numerical errors associated with this method. The CVFE method produces an estimate, which is close (12%) to the true value. Comparing just the VFG and FG results (cases 1 and 2 in Table 6), we might assume that the grid resolution does not substantially impact the inverse estimates. However, including the CG (case 3) result in this comparison, we conclude that the grid resolution effect is very important.

Table 5
Parameters and Grid Characteristics for Two-Dimensional Problem of Unsaturated Flow through a Layered Medium

Problem size (m)	X direction 10,000
	Z direction 1700
Specified fluxes (inflow) (kg/s)	0.1 (inflow 1)
	0.2 (inflow 2)
Outflow head condition (m)	700
Permeabilities (m²)	10^{-12} (zone 1)
Very fine scale values	5×10^{-16} (zone 2)
	10^{-13} (zone 3)
Porosity	0.2
Capillary pressure model	Linear
Maximum capillary	0.1 (zone 1)
pressure (MPa)	1.0 (zone 2)
	0.1 (zone 3)
Relative permeability model	Linear with saturation
	(all zones)
Grid resolution (m)	X direction 25
(very fine scale)	Z direction 25

Table 6
**Permeability Estimates Obtained Using Different Grid Resolution and Differencing Techniques for a
Two-Dimensional Variably Saturated Flow through a Layered Medium**

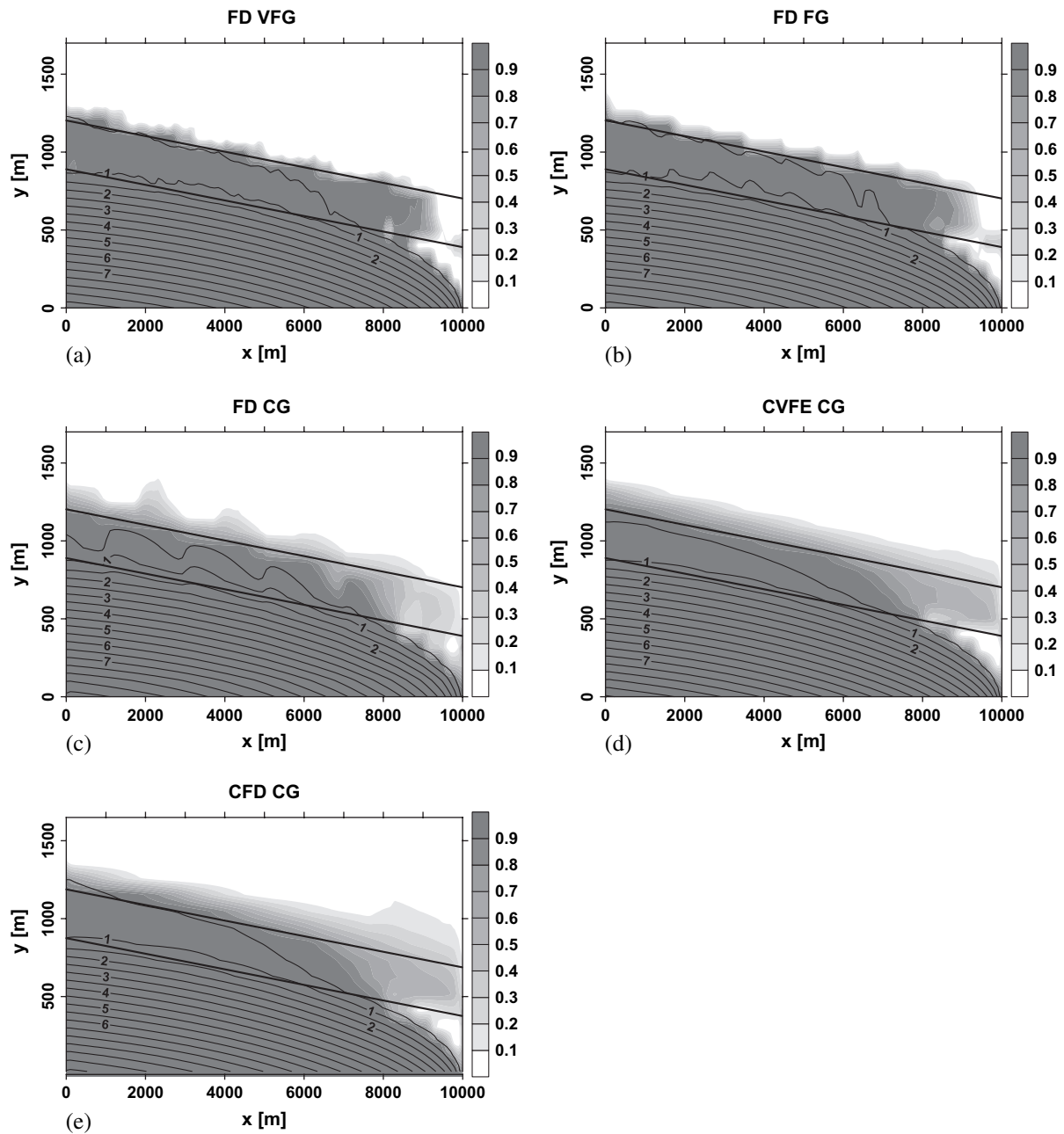| Case	Grid	Method	Number of Grid Blocks	(DX, DZ) (m)	k (zone 1) (m²)	k (zone 2) (m²)	k (zone 3) (m²)	SSR (m²)
1	VFG	FD	27,336	(25, 25)	1.0×10^{-12} (truth)	5.0×10^{-16} (truth)	1.0×10^{-13} (truth)	…
2	FG	FD	6868	(50, 50)	1.4×10^{-12}	5.4×10^{-16}	9.8×10^{-14}	0.125
3	CG	FD	1734	(100, 100)	1.2×10^{-11}	6.4×10^{-16}	1.0×10^{-13}	1.29
4	CG	CFD	1734	(100, 100)	5.1×10^{-13}	4.1×10^{-16}	8.8×10^{-14}	2.07
5	CG	CVFE	1836	(100, 100)	8.8×10^{-13}	4.4×10^{-16}	8.5×10^{-14}	3.61

Figure 6. Two-dimensional flow solutions of the layered variable-saturation problem for the different inverse models: (a) FD VFG, (b) FD FG, (c) FD CG, (d) CVFE CG, and (e) CFD CG. The distributions of water saturation (gray scale) and hydraulic pressure (MPa, lines) within the model domain are presented: Thick lines show the location of the slanted low-permeable layer in the middle of the domain.

Figure 6 represents the impact of differencing techniques and grid resolution on the ground water flow. Comparing the FD solutions, we note that the grid resolution affects the smoothness of the water table and top of the saturated zone (stair-step behavior). Compared to the VFG finite-difference case, the FG and CG finite-difference solutions are not very accurate in the representation of the saturation in the right end of layer 2. The coarse-grid CFD and CVFE methods nicely represent the perching associated with zone 2 though they are also (as coarse-grid FD) overestimating the saturation in the right end of layer 2. However, as we mentioned previously, CFD achieves this introducing a substantial bias in the inverse estimates.

As mentioned in the Introduction, a flow model is often used for transport calculations once it is calibrated with field data. One transport example is given for the saturated/unsaturated zone example to illustrate the effect of the differencing methods. Figure 7 shows the relative concentrations of a contaminant introduced in the system as a constant concentration source along the top right boundary of the model domain (see Figure 5). The contour plots shown are for the same simulated time 500 d after the introduction of the contaminant. Results are similar overall for the CFD and CVFE methods.

However, model-predicted distributions of contaminants based on the CFD and CVFE solutions are different. Comparing Figures 7c and 7d, it can be seen that the CFD solution has higher concentrations near the left side and is more diffuse that the CVFE results. For example, the relative concentration of 0.6 is at $x \approx 6000$ m for the CFD case and at $x \approx 5200$ m for the CVFE case. A substantial grid effect (stair-step behavior) is produced by the FD, method although the concentration front (say ~0.5) is close to that of the CVFE method.

Summary, Conclusions, and Recommendations

We summarize the results as follows:

- The transient well problem shows that, based purely on grid resolution, permeability estimates can be in error by several hundred percent. A judicious choice of variable grid spacing can easily minimize the error.
- For fully saturated ground water flow with sloping permeability structure, it is more important, with the coarsest grid resolution, to capture the permeability fields with a conforming grid than using a standard orthogonal grid and representing the permeability in a stair-step manner. The coarse standard FD grid constricted flow in the
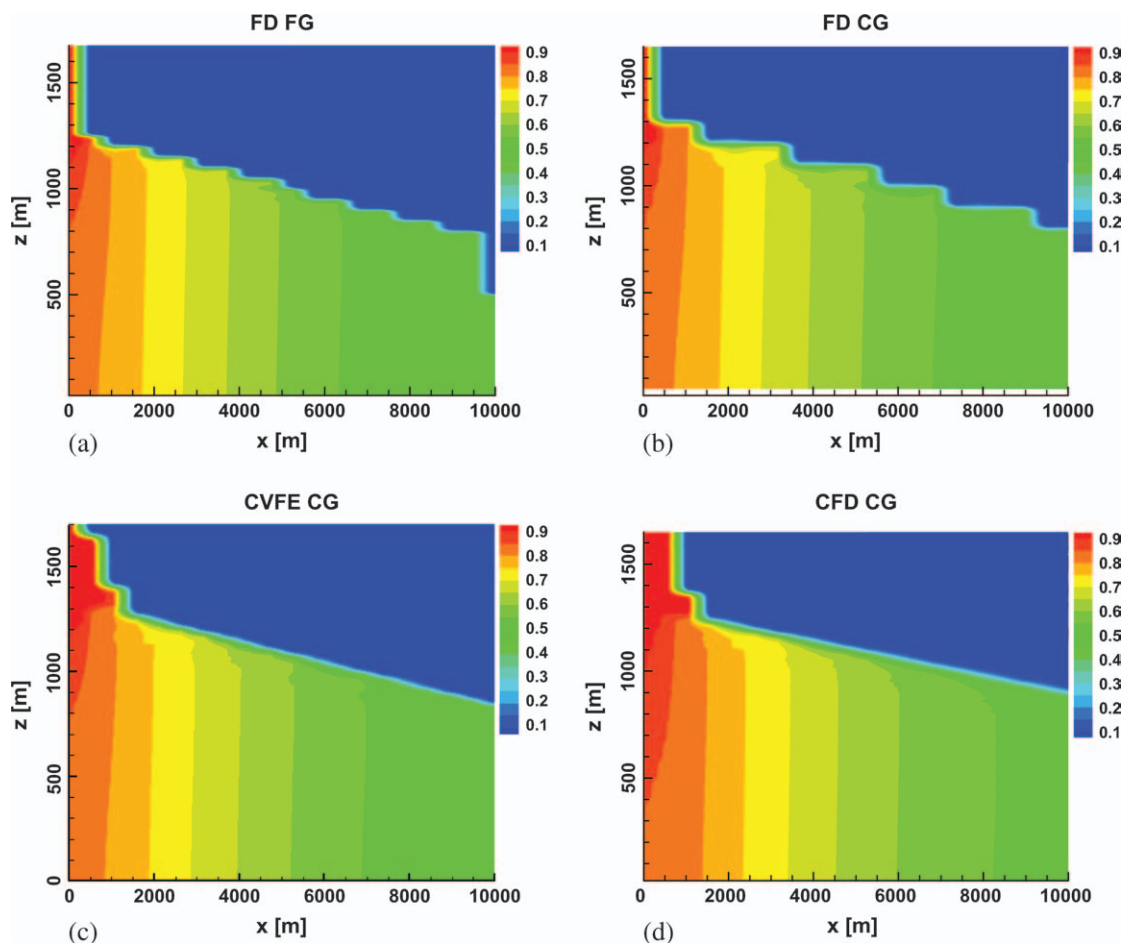

Figure 7. Two-dimensional transport solutions of the layered variable-saturation problem for the different inverse models: (a) FD FG, (b) FD CG, (c) CVFE CG, and (d) CFD CG. The relative concentration of contaminants is presented using color-coded contours. The figures represent concentration distribution 500 d after the release. The underlying flow solution is at steady state.

medium permeability unit where fluid was injected in the test example. To compensate, estimated permeabilities are 20 to 80 times higher than actual values. The CFD method cures this problem and incurs only small errors. The CFD solution is equivalent in estimation accuracy to the CVFE solution except on the coarsest grid where its estimate is ~20% poorer.

- For the unsaturated zone problems, CFD methods produce solutions for the spatial distribution of saturation and hydraulic pressure that are qualitatively better than those obtained by the standard differencing methods using the same grid resolution. While the coarse standard FD solution overestimates the permeability of one of the layers by almost a factor of 10, the CFD solution underestimates the permeability by a factor of 5. The CVFE solution was the most accurate, and underestimated permeability for the same unit by only 12%.
- Impact of the inaccurate inverse estimates based on the inverse flow model might be very pronounced for the ground water transport simulations based on the calibrated model.

Grid resolution and differencing formulation were found to be important to inverse estimates of model parameters. There are tradeoffs between errors in differencing methods and crude representation of hydrostratigraphy. These factors in turn affect the CPU requirements of each method. The authors analyzed the CPU and memory requirements of FD and CVFE methods on a large regular grid test problem, which is described in Appendix 1. We estimate the additional complexity of the CVFE results in the method having CPU times ~1.5 times greater than FD or CFD methods when run on the identical problem. When off-diagonal terms arise because of a sloping grid, the addition of 50% more connections (for the problems herein) will lead to an estimated $1.5 \times 1.1 = 1.65$ increase in CPU time. An absolute performance measure for each method is beyond the scope of this study. Besides the usual CPU increase with problem size, the nonlinear unsaturated zone problems also saw an increase, with problem size, in the number of time steps necessary to obtain a steady-state solution. Also, the number of model runs to obtain a calibrated model varied with problem size. In terms of accuracy of parameter estimates, the standard FD solution usually was the worst of the three numerical schemes; however, its estimates improved dramatically with increasing grid resolution. CFD methods, because of the systematic grid angle error, are not as amenable to this type of study and were difficult to judge. Nevertheless, conforming difference methods appear to be useful in fully saturated flow simulations when the slope of the boundaries between different hydrostratigraphic units is moderate (as the 5% slope analyzed in the study). The authors suspect that the appropriate use of CFD methods depends on the slope angle, the ratio of vertical to horizontal ground water flux, and the permeability contrast of the layers. We advise caution in the use of conforming methods for unsaturated zone work or simulations involving an unsaturated zone or a movable water table. Because of the accuracy and versatility of CVFE methods (noting the extra CPU and memory requirements), we recommend their use in all problems. In some cases such as the saturated zone example presented here, inaccurate representation of the geometry of the hydrostratigraphic units in the model may have an overwhelming effect compared to other numerical errors introduced by the computational grid. In other cases, such as the unsaturated zone example presented here, there was an advantage in using conforming layers in the coarsest grid; however, the errors were larger than might be expected on a mildly sloping grid. The errors were also considerably higher than the CVFE solution. Inaccurate inverse estimates based on the flow model may cause pronounced effects on transport simulations.

Though we have not rigorously analyzed the saturated zone transport case, we suspect errors similar to those encountered when solving the unsaturated flow equations. An upwinded (first-order accurate) formulation was used to model the concentration front in much the same way as the upwinded relative permeabilities are used in the simulation on the saturation front. Detailed analysis will have to wait for a subsequent paper.

The proposed methodology can be used to test the impact of grid on the inverse model estimates before the model is calibrated to the real data. A priori grid testing, like that done by Bower et al. (2004), can suggest an appropriate grid resolution for accurate inverse studies.

Acknowledgments

Appendix 1

Discussion of Model Run Times and Memory Requirements

Because this paper discusses the relative merits of the CVFE, CFD, and FD methods, the CPU time and memory requirements should be compared. However, the authors did not have at their disposal a CVFE computer code designed to solve isothermal ground water problems. Nevertheless, the authors used a test case based on a problem from Mehl and Hill (2002; problem 1, case 1) and compared run times from codes FEHM and MODFLOW (version MF2K1.13, compiled in double precision) that implement these methods. The test problem is simple and represents a producing well in a homogeneous media. The problem consists of ~1.1 million grid blocks and is run to steady state. The authors ran this problem using FEHM and MODFLOW using comparable preconditioner complexity and stopping criteria. Listed in Table A1 are the run times. This problem took 125 s of CPU time for MODFLOW and 130 s of CPU time for FEHM when run on a Dell 650 Workstation with a 3-GHz

Table A1
Comparison of CPU and Memory Requirements for CVFE and FD Methods

Method[1]	Ax = b (solver storage)	Storage for Coordinates	Connectivity[2]	Area Array (stiffness array)	CPU Time	RAM
CVFE	2(equations) + 2(preconditioner)	1	1/2(equations) + 1/2(preconditioner)	1	130 s (FEHM)	1.37 gigabyte (FEHM)
FD	1(equations) + 1/2(preconditioner)	0	0	0	125 s (MODFLOW)	0.17 gigabyte (MODFLOW)

[1]Theoretical memory requirements estimated in Multiples of Solution Matrix for symmetric problem ($\sim 3N$, N is the number of grid blocks).
[2]1/2 represents a real-word equivalent for an integer array.

Intel processor. It is unclear whether the speed difference is due to the properties of solution matrices (nonsymmetric vs. symmetric), solver method, or indirect addressing and unstructured connectivities in the case of CVFE (FEHM).

Since this paper concerns a comparison on CVFE and FD (CFD and FD have the same CPU and memory requirements) methods in general rather than their code-particular implementation, we have attempted to compare the memory requirement of methods based on a theoretical basis as well as the actual memory required for FEHM and MODFLOW. We note that FEHM solves the test problem describing confined, fully saturated flow using nonsymmetric solution matrices, while MODFLOW uses a symmetric approach. FEHM uses nonsymmetric solution matrices to accommodate requirements from other physics packages built in the code that are nonlinear. Compared to MODFLOW, FEHM also uses additional storage arrays, among other things, for temperature-dependent density and viscosity, storage for Newton-Raphson iterations, and sophisticated pressure-dependent porosity models, and double/dual porosity capability. The major memory requirements are also listed in Table A1. For the problem listed previously, MODFLOW used ~0.17 gigabyte of memory, FEHM used ~1.4 gigabyte of memory, about a factor of 8 difference in the memory requirements. We also estimated theoretical memory requirements based on only the ground water equations that MODFLOW solves and restricted this estimate to a two-dimensional problem. Here, the connectivity (9 point vs. 5 point) makes the solution array **A** (as in **Ax = b**) about twice as large. The interface area array (similar to the finite-element stiffness matrix) adds computer storage equal to the solution array. The grid block coordinates, which must be explicitly entered for the CVFE method, add storage equal to the solution array. The preconditioner for the solution of the matrix equations is also twice as large in the case of CVFE. Finally, due to the unstructured nature of the CVFE method, two integer pointer arrays (equal in size to the solution array) are required: one for the grid block connectivity and one for the solver preconditioner connectivity. Based on these considerations, a "theoretical" CVFE code with capabilities similar to MODFLOW is estimated to need ~3.5 times the MODFLOW memory.

References

Barlow, P.M. 1994. Two- and three-dimensional pathline analysis of contributing areas to public-supply wells of Cape Cod, Massachusetts. *Ground Water* 32, no. 3: 399–410.

Bower, K.M., C. Gable, and G. Zyvoloski. 2005. Grid resolution study of ground water flow and transport, Yucca Mountain. *Ground Water* 43, no. 1: 122–132.

Carrera, J. 1984. Estimation of aquifer parameters under transient and steady state conditions. Ph.D. diss., Department of Hydrology and Water Resources, University of Arizona, Tucson, Arizona.

Cole, C.R., S.K. Wurstner, M.D. Williams, P.D. Thorne, and M.P. Bergeron. 1997. Three-dimensional analysis of future groundwater flow conditions and contaminant plume transport in the Hanford Site unconfined aquifer system; FY 1996 and 1997 status report. Report PNNL-11801. Pacific Northwest National Laboratory, Hanford, Washington.

de Marsily, G., J.P. Delhomme, A. Coudrain-Ribstein, and A.M. *Lavenue*. 2000. Four decades of inverse problems in hydrogeology. *Geological Society of America Special Papers* 348: 1–17.

Doherty, J. 2000. *PEST-Model Independent Parameter Estimation*. Corinda, Australia: Watermark Computing.

Flach, G.P., L.L. Hamm, M.K. Harris, P.A. Thayer, J.S. Haselow, and A.D. Smits. 1996. Groundwater flow and tritium migration from the SRS Old Burial Ground to four mile branch (U). Technical Report No. WSRC-TR-96-0037. Westinghouse Savannah River Company, Aiken, South Carolina.

Forsyth, P.A. 1989. A control volume finite element method for local mesh refinement. SPE 18415 presented at the Tenth SPE Symposium on Reservoir Simulation, February 6–8, Houston, Texas.

Gaganis, P., and L. Smith. 2001. A Bayesian approach to the quantification of the effect of model error on the predictions of ground water models. *Water Resources Research* 37, no. 9: 2309–2322.

George, D.C., A. Kuprat, N.N. Carlson, and C.W. Gable. April 1999. LaGrit-Los Alamos Grid Tool, http://lagrit.lanl.gov, LA-CC-99-0017.

Harte, P.T. 1994. Comparison of vertical discretization techniques in finite-difference models of ground-water flow: Example from a hypothetical New England setting. USGS Open-File Report 94-343.

Hoagland, J.R., and D. Pollard. 2003. Dip and anisotropy effects on flow using a vertically skewed model grid. *Ground Water* 41, no. 6: 841–846.

Kautsky, M., B. Smith, R. Zinkl, and D. Metzler. 2001. The use of 'Conformable Layers' to model sites with high relief. In *MODFLOW 2001 and Other Modeling Odysseys*, eds. E.P. Poeter, C. Zheng, and M.C. Hill, September 11–14. Golden, Colorado.

Keating, E.H., V.V. Vesselinov, E. Kwicklis, and Z. Lu. 2003 Coupling large- and local-scale inverse models of the Española basin. *Ground Water* 41, no. 2: 200–211.

Lee S.H., H. Tchelepi, and L.F. De Chant. 1999. Implementation of a flux-continuous finite difference method for stratigraphic, hexahedron grids. SPE 51901 presented at the Fifteenth SPE Symposium on Reservoir Simulation, February 14–17, Houston, Texas.

Lemon, A.M., and N.L. Jones. 2001. Managing complex stratigraphy in MODFLOW models. In *MODFLOW 2001 and Other Modeling Odysseys*, eds. E.P. Poeter, C. Zheng, and M.C. Hill, September 11–14. Golden, Colorado.

Liu, J., E.L. Sonnenthal, and G.S. Bodvarsson. 2003. Calibration of Yucca Mountain unsaturated zone flow and transport using porewater chloride data. *Journal of Contaminant Hydrology* Apr-May, 62, 213–236.

McDonald, M.G., and A.W. Harbaugh. 1988. A modular three-dimensional finite-difference ground-water flow model. In *U.S. Geological Survey Techniques of Water-Resources Investigations* book 6, chap. A1. Denver, Colorado: USGS.

McLaughlin, D., and L.R. Townley. 1996. A reassessment of the ground water inverse problem. *Water Resources Research* 32, no. 5: 1131–1161.

Mehl, S.W., and M.C. Hill. 2002. Development and evaluation of a local grid refinement method for block-centered finite-difference groundwater models using shared nodes. *Advances in Water Resources* vol. 25, 497–511.

Neuman, S.P. 2003. Accounting for conceptual model uncertainty via maximum likelihood Bayesian model. In *ModelCARE 2002 Calibration and Reliability in Groundwater Modelling: A Few Steps Closer to Reality*, eds. K. Kovar and Z. Hrkal, 303–313. IAHS Publication 277. Prague, Czech Republic, Acta Universitatis Carolinae-Geologica 2002, 46.

Neuman, S.P. 1976. *User's Guide for FREESURF I.* Tucson, Arizona: Department of Hydrology and Water Resources, University of Arizona.

Neuman, S.P., and P.A. Witherspoon. 1970. Finite element method of analyzing steady seepage with a free surface. *Water Resources Research* 6, no. 3: 889–897.

Rehfeldt, K.R., J.M. Boggs, and L.W. Gelhar. 1992. Field study of dispersion in a heterogeneous aquifer. 3: Geostatistical analysis of hydraulic conductivity. *Water Resources Research* 28, no. 12: 3309–3324.

Rozon, B.J. 1989. A generalized finite volume discretization method for reservoir simulation. SPE 18414 presented at the Tenth SPE Symposium on Reservoir Simulation, February 6–8, Houston, Texas.

Sinton, P.O. 1998. Problems applying MODFLOW-Style models to three-dimensional flow. In *Proceedings of the 25th Annual Conference on Water Resources Planning and Management*, ed. W. Whipple, June 7–10, 655–660. Chicago, Illinois: American Society of Civil Engineers.

Weiss, E. 1985. Evaluating the hydraulic effects of changes in aquifer elevation using curvilinear coordinates. *Journal of Hydrology* 81: 253–275.

Young, L.C. 1999. Rigorous treatment of distorted grids in 3D. SPE 51899 presented at the Fifteenth SPE Symposium on Reservoir Simulation, February 14–17, Houston, Texas.

Zyvoloski, G.A., E. Kwicklis, A.A. Eddebbarh, B. Arnold, C. Faunt, and B.A. Robinson. 2003. The site-scale saturated zone flow model for Yucca Mountain: Calibration of different conceptual models and their impact on flow paths. *Journal of Contaminant Hydrology* Apr-May, 62, 731–750.

Zyvoloski, G.A., B.A. Robinson, Z.V. Dash, and L.L. Trease. 1997. User's manual for the FEHM application—A finite-element heat- and mass-transfer code LA-13306-M. Los Alamos, New Mexico: Los Alamos National Laboratory.